THE EFFECT OF MASS TRANSFER ON MULTI-SPAN LATERAL DYNAMICS OF NONUNIFORM WEBS

By

Jerald L. Brown
Essex Systems
USA

ABSTRACT

Since the publication of Shelton's original work [1] on lateral web dynamics in 1968, the cambered[1] web has attracted the attention of researchers. Shelton, himself, felt it was a natural "next step" in lateral dynamics. It is not only interesting as a theoretical challenge. It is the simplest case of an important class of lateral handling problems known as baggy[2] webs. However, despite considerable effort by many people, it is still considered by many authorities in the field to be an unsolved problem.

In a companion paper, presented at this conference [2], concepts based on mass flow were used to resolve difficulties with uniform web models that included shear deformation. This paper will show that these ideas, when combined with methods introduced by Linda Sievers [3], can resolve one of the most significant issues with cambered web models – the question of the 4th boundary condition.

The 4th boundary condition refers to one of the two relationships at the downstream end of a web span (the other two are at the upstream end). For uniform webs in a steady state without shear, this is a settled issue. Shelton found that it was zero moment and verified it experimentally. The other relationship at the downstream end, called the normal entry rule, is well known and generally accepted. It specifies that the web centerline will be normal to the roller axis.

In dynamic uniform web models, the 4th boundary condition takes the form of a relationship between curvature and acceleration that obligingly defaults to the zero-moment condition when the time-based terms decay to zero.

---

[1] A web that has constant lateral curvature in its relaxed state. It forms an arc when laid flat on a floor.

[2] A web that has slack lanes when running under tension. A cambered web is the simplest example. In the worst cases, the web is so deformed that relaxed samples will not even lay flat. The usual strategy for dealing with it is to increase tension to "pull out" the baggy lanes, but the required level may be so high that it either damages the web or causes other problems, such poor winding conditions.

In 2002, Richard Benson published a paper [4] that is similar in some respects to the method discussed here. Although there is no mention of mass flow, he found and applied a key relationship that enforces its effects. He found the relationship by assuming that the rotational velocity of the bending angle of the web must match the pivoting velocity of the roller at the downstream end of a span. Using this, he developed a cambered web model similar to the one described here. However, he incorrectly concluded that camber has no effect on lateral behavior because he overlooked its effects on the boundary conditions.

Benson also derived an acceleration equation for uniform webs that correctly incorporates shear.

NOMENCLATURE

A	cross sectional area of web
E	elastic modulus
G	shear modulus
h	thickness of web
I	area moment of inertia
L	span length
n	Shear factor for Timoshenko beam
N	Side force
s	Laplace variable
t	time
T	tension in units of force
V_o	web velocity in machine direction
x	distance along length of web
y	lateral displacement of web
y_0	lateral web displacement at upstream roller, relative to ground
y_L	lateral web displacement at downstream roller, relative to ground
z	lateral displacement of roller relative to ground
θ_L	angle between web plane and plane of roller motion at entry to roller
θ_0	angle between web plane and plane of roller motion at exit of roller
β	boundary defect angle
γ	angle of roller axis
ρ	density
ϕ	bending angle (rotation of cross section or face angle)
ψ	shear angle
χ	shape angle (slope of relaxed web)
$_0$	subscript indicating value of variable at $x = 0$
$_L$	subscript indicating value of variable at $x = L$

INTRODUCTION

<u>Outline of the Method</u>

This paper will develop a cambered web model using the following key ideas.

1) Recognition that the slope of the centerline is the sum of bending and shear angles plus the slope of the relaxed curve of the web. This may seem trivial, but it has not

been obvious to many of the earlier researchers and it is central to the method used here.

2) Use of the calculus of variations (either Hamilton's principle or virtual work) to generate the 4^{th} order ordinary differential equation defining the elastic curve of the web.
3) Solution of the ODE of step 2 for lateral position – an equation with four unknown coefficients and three hyperbolic functions of position *x* along the span,
4) Application of boundary conditions (bending angle and lateral position at the upstream end; bending angle and lateral position at the downstream end) to the equation of step 3 to solve for the four coefficients.
5) Conversion of the equation for the elastic curve of step 4 to a 2^{nd} order time-based ordinary differential equation by converting slope and curvature at the downstream end to velocity and acceleration using,
   a) The normal entry equation (velocity)
   b) The mass transfer equation (acceleration)
6) Careful development of boundary conditions that takes account of the fact that the shape angle is discontinuous at rollers.

Shelton [1] was the first to apply beam theory to the analysis of lateral web dynamics and pioneered many of the methods we still use today. He developed both steady state and dynamic models based on Euler-Bernoulli theory. These were verified by experiment. He also developed a steady state model that correctly incorporated shear, but was unsuccessful with efforts to develop a dynamic shear model

Sievers [3] was the first to make steps 1, 2 and 4 central features of beam modeling.

MODELING THE CAMBERED WEB

The Elastic Curve

The first step is to define the slope of the web as the sum of bending, shear angles plus the slope of the relaxed web shape. Thus,

$$\frac{dy_L}{dx} = \phi + \psi + \chi \quad , \qquad \{1\}$$

where, ϕ is the bending angle, ψ is the shear angle and χ is the shape angle of the relaxed web and,

$$\chi = \frac{d}{dx} f(x) \quad , \qquad \{2\}$$

where *f(x)* is the lateral displacement of the relaxed web – the nonuniformity.

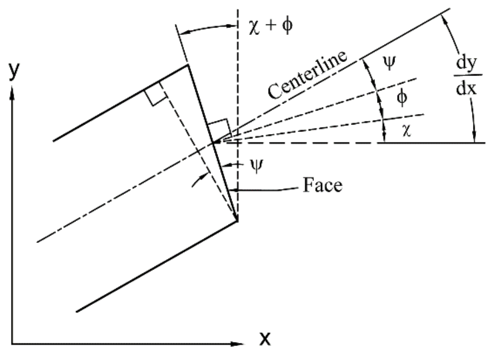

Figure 1 –Relationships between Slope, Shear, Bending Angle and Shape Angle

The next step is to define the elastic strain energy for the web, Π.

$$\Pi = \int_0^L \left[\frac{1}{2} EI \left(\frac{d\phi}{dx} \right)^2 + \frac{1}{2} \frac{GA}{n} \psi^2 + \frac{1}{2} T \left(\frac{dy}{dx} \right)^2 \right] dx \tag{3}$$

In this equation, *E* is the modulus of elasticity, *I* is the area moment of inertia, *G* is the shear modulus, *A* is the cross sectional area and *T* is the tension. The factor, *n*, comes from Timoshenko beam theory and accounts for the fact that the shear stress is assumed to be a uniform average value across the width of the web. For a rectangular profile, it is approximately 1.2.

Using {1} to eliminate ψ and applying the method of virtual work to Π yields for the variation with respect to ϕ[3].

$$\delta \Pi_\phi = \int_0^L \delta\phi_x \frac{\partial}{\partial \phi_x} \left[\frac{1}{2} EI \left(\phi_x \right)^2 \right] dx + \int_0^L \delta\phi \frac{\partial}{\partial \phi} \left[\frac{1}{2} \frac{GA}{n} \left(y_x - \phi - \chi \right)^2 \right] dx = 0 \tag{4}$$

Integrating {4} by parts (twice for the first integral on the right),

$$\delta \Pi_\phi = \left[\delta\phi EI \frac{d\phi}{dx} \right]_0^L - \int_0^L \delta\phi \left[EI \frac{d^2\phi}{dx^2} + \frac{GA}{n} \left(\frac{dy}{dx} - \phi - \chi \right) \right] dx = 0 \tag{5}$$

The variation with respect to *y* is,

$$\delta \Pi_y = \int_0^L \delta y_x \frac{\partial}{\partial y_x} \left[\frac{1}{2} \frac{GA}{n} \left(y_x - \phi - \chi \right)^2 \right] dx + \int_0^L \delta y_x \frac{\partial}{\partial y_x} \left[\frac{T}{2} \left(y_x \right)^2 \right] dx = 0 \tag{6}$$

Integrating both integrals of {6} by parts twice,

$$\delta \Pi_y = \left[\delta y \left(\frac{GA}{n} \left(\frac{dy}{dx} - \phi - \chi \right) + T \frac{dy}{dx} \right) \right]_0^L - \int_0^L \delta y \left[\frac{GA}{n} \left(\frac{d^2 y}{dx^2} - \frac{d\phi}{dx} - \frac{d}{dx} \chi \right) + T \frac{d^2 y}{dx^2} \right] dx = 0 \tag{7}$$

[3] For convenience in notation, ϕ_x is used to represent *dϕ/dx* and y_x represents *dy/dx*.

Variation with respect to χ isn't needed because there is no energy associated with it by itself. Its effects are recognized in the other variations.

The variations $\delta\phi$ and δy in {5}and {7} must be zero at $x = 0$ and $x = L$. At other values of x they are arbitrary. Therefore, for $\delta\Pi_\phi = \delta\Pi_y = 0$, the quantities inside the brackets under the integrals must be zero. These are the equations that govern the shape of the elastic curve of a nonuniform web.

$$\left(\frac{nT}{AG}+1\right)\frac{d^2y}{dx^2} - \frac{d\phi}{dx} - \frac{d\chi}{dx} = 0 \qquad \{8\}$$

$$EI\,\frac{d^2\phi}{dx^2} + \frac{AG}{n}\left[\frac{dy}{dx} - \phi - \chi\right] = 0 \qquad \{9\}$$

These equations can be expressed as a single 4th order equation in y by first differentiating {9}. Then, expressions for $d\phi/dx$ and $d^2\phi/dx^2$ are calculated using {8} and substituted into {9}. The result is,

$$\frac{d^4y}{dx^4} - K^2\,\frac{d^2y}{dx^2} = \frac{1}{a}\,\frac{d^3}{dx^3}\chi \qquad \{10\}$$

where,

$$K = \sqrt{\frac{T}{EIa}} \qquad \{11\}$$

and

$$a = \left(1+\frac{Tn}{AG}\right) \qquad \{12\}$$

Additionally, it can be shown that shear force, N, moment, M and bending angle, ϕ, are,

$$N = EI\,\frac{d^2\phi}{dx^2} = EI\left[a\frac{d^3y}{dx^3} - \frac{d^2\chi}{dx^2}\right] \qquad \{13\}$$

$$M = EI\,\frac{d\phi}{dx} = EI\left[a\frac{d^2y}{dx^2} - \frac{d\chi}{dx}\right] \qquad \{14\}$$

$$\phi = \frac{EI}{AG}\left(a\frac{d^3y}{dx^3} - \frac{d^2}{dx^2}\chi\right) + \frac{dy}{dx} - \chi \qquad \{15\}$$

Cambered Web

The arc of a cambered web can be approximated as a shallow parabola,

$$f(x) = \frac{\left(x - x_o\right)^2}{2R_w} \qquad \{16\}$$

where x_o is a constant that controls the x-location of the center of the arc and R_w is the radius of curvature. So, for a cambered web,

$$\frac{d^4y}{dx^4} - K^2\frac{d^2y}{dx^2} = 0 \qquad \{17\}$$

and,

$$\phi = \frac{EI}{AG}a\frac{d^3y}{dx^3} + \frac{dy}{dx} - \frac{x-x_o}{R_w} \qquad \{18\}$$

$$N = EI\frac{d^2\phi}{dx^2} = EIa\frac{d^3y}{dx^3} \qquad \{19\}$$

$$M = EI\frac{d\phi}{dx} = EI\left[a\frac{d^2y}{dx^2} - \frac{1}{R_w}\right] \qquad \{20\}$$

The moment equation makes sense when it is realized that, the curvature term $a(d^2y/dx^2)$ includes the purely geometric effect of the relaxed curvature of the web. So, to calculate the bending moment, the fixed curvature, $1/R_w$, must be subtracted from it.

The solution to {17} is the familiar result,

$$y(x) = C_1\sinh(Kx) + C_2\cosh(Kx) + C_3x + C_4 \qquad \{21\}$$

It may seem strange that {17}is the same as for a uniform web. Where did the camber go? It is partly the victim of the underlying approximations of beam theory. They are implicit in the definitions of energy that got us here. The effects of camber, which intuition tells us must exist, will be evident in the effects of the boundary conditions on the coefficients of {21} – primarily the moment and bending angle equations {20} and {18}.

<u>Boundary Conditions for the Elastic Curve</u>

As in the uniform web model, the interaction of the web with rollers is greatly simplified. The width of the contact zone in the process direction is assumed to be zero.

Lateral positions at the upstream and downstream rollers will provide two of the four required boundary conditions. Following the example of the uniform web, the bending angles are chosen for the other two.

So, the boundary conditions for the cambered web (including shear deformation) are,

$$\begin{aligned} &y\big|_{x=0} = y_0 && y\big|_{x=L} = y_L \\ &\left.\frac{dy}{dx}\right|_{x=0} + EIa\frac{n}{AG}\left.\frac{d^3y}{dx^3}\right|_{x=0} - \chi_0 = \phi_0 && \left.\frac{dy}{dx}\right|_{x=L} + EIa\frac{n}{AG}\left.\frac{d^3y}{dx^3}\right|_{x=L} - \chi_L = \phi_L \end{aligned} \qquad \{22\}$$

where,

$$\chi(0) = \left.\frac{df(x)}{dx}\right|_{x=0} = \chi_0 = \frac{-x_o}{R_w} \quad and \quad \chi(L) = \left.\frac{df(x)}{dx}\right|_{x=L} = \chi_L = \frac{L-x_o}{R_w} \qquad \{23\}$$

Equations {21} and its derivatives are substituted into the four equations of {22} which are then solved simultaneously for C_1, C_2, C_3 and C_4.

The Static Equation of Web Shape

Inserting values {22} into {21} and collecting terms,

$$y(x) = y_0 + \left(y_0 - y_L\right) g_4(x) + \left[\phi_L + \chi(L)\right] g_5(x) + \left[\phi_0 + \chi(0)\right] g_6(x) \qquad \{24\}$$

where,

$$\begin{aligned} g_4(x) &= \frac{\cosh(Kx)+\cosh(KL)-\cosh(KL-Kx)-Kax\sinh(KL)-1}{KLa\sinh(KL)-2\left(\cosh(KL-1\right)} \\ g_5(x) &= \frac{KLa\left(\cosh(Kx)-1\right)-Kax\left(\cosh(KL)-1\right)-\sinh(Kx)-\sinh(KL-Kx)+\sinh(KL)}{Ka[KLa\sinh(KL)-2\left(\cosh(KL-1\right)]} \\ g_6(x) &= \frac{\sinh(Kx)-\sinh(KL)+\sinh(KL-Kx)-KLa\left(\cosh(KL-Kx)-1\right)+Ka(L-x)(\cosh(KL)-1)}{Ka[KLa\sinh(KL)-2\left(\cosh(KL-1\right)]} \end{aligned} \qquad \{25\}$$

Three other equations that will be needed later are the first, second and third derivatives of {21} at $x = L$.

$$\left.\frac{dy(x)}{dx}\right|_L = \left(y_0 - y_L\right)\frac{h_1}{L} + \left[\phi_L + \chi(L)\right] h_2 + \left[\phi_0 + \chi(0)\right] h_3 \qquad \{26\}$$

$$\left.\frac{d^2y(x)}{dx^2}\right|_L = \left(y_0 - y_L\right)\frac{g_1}{L^2} + \left[\phi_L + \chi(L)\right]\frac{g_2}{L} + \left[\phi_0 + \chi(0)\right]\frac{g_3}{L} \qquad \{27\}$$

$$\left.\frac{d^3y(x)}{dx^3}\right|_L = \left(y_0 - y_L\right)\frac{f_1}{L^3} + \left[\phi_L + \chi(L)\right]\frac{f_2}{L^2} + \left[\phi_0 + \chi(0)\right]\frac{f_3}{L^2} \qquad \{28\}$$

where,

$$\begin{aligned} h_1 &= \frac{KLa\sinh(KL)(1-a)}{a\left[KLa\sinh(KL)-2\left(\cosh(KL)-1\right)\right]} \\ h_2 &= \frac{(a+1)\left(1-\cosh(KL)\right)+KLa\sinh(KL)}{a\left[KLa\sinh(KL)-2\left(\cosh(KL)-1\right)\right]} \\ h_3 &= \frac{(a-1)\left(1-\cosh(KL)\right)}{a\left[KLa\sinh(KL)-2\left(\cosh(KL)-1\right)\right]} \end{aligned} \qquad \{29\}$$

$$\begin{aligned} g_1 &= \frac{K^2L^2a\left(\cosh(KL)-1\right)}{a\left[KLa\sinh(KL)-2\left(\cosh(KL)-1\right)\right]} \\ g_2 &= \frac{KL\left(KLa\cosh(KL)-\sinh(KL)\right)}{a\left[KLa\sinh(KL)-2\left(\cosh(KL)-1\right)\right]} \\ g_3 &= \frac{KL\left(\sinh(KL)-KLa\right)}{a\left[KLa\sinh(KL)-2\left(\cosh(KL)-1\right)\right]} \end{aligned} \qquad \{30\}$$

$$f_1 = \frac{K^3L^3 a\sinh(KL)}{a\left[KLa\sinh(KL)-2\left(\cosh(KL)-1\right)\right]}$$
$$f_2 = \frac{K^2L^2\left(1-\cosh(KL)+KLa\sinh(KL)\right)}{a\left[KLa\sinh(KL)-2\left(\cosh(KL)-1\right)\right]} \qquad \{31\}$$
$$f_3 = \frac{K^2L^2\left(\cosh(KL)-1\right)}{a\left[KLa\sinh(KL)-2\left(\cosh(KL)-1\right)\right]}$$

Note that the constants of {25}, {29}, {30} and {31} are the same as for a uniform web.

In the models where shear is insignificant ($nT/AG = 0$), $a = 1$ and that in turn causes $h_1 = h_3 = 0$ and $h_2 = 1$. This reduces {26} to,

$$\left.\frac{dy(x)}{dx}\right|_L = \phi_L + \chi_L \qquad \{32\}$$

THE TIME EQUATIONS THAT CONVERT THE STATIC WEB SHAPE TO A DYNAMIC EQUATION[4]

The Velocity Equation

There is no reason why the velocity equation for uniform and nonuniform webs should not be the same. So,

$$\frac{dy_L}{dt} = V_o\left(\gamma_L - \frac{dy_L}{dx}\right) + \frac{dz_L}{dt} \qquad \{33\}$$

The first group of terms on the right side is the lateral velocity due to the interaction of surface velocity of the roller and the slope of the web. The quantity inside the parenthesis is called the entry angle. The last term is the lateral velocity of the roller itself. The velocity term on the left is the lateral velocity of the web relative to ground. It is important to remember that {33} is true only at $x = L$ and should not, therefore, be differentiated with respect to x.

The Acceleration Equation

Following the example of uniform web analysis [2], the mass transfer concept is used to develop an acceleration equation. In the discussion of qualitative behavior that follows, it will be assumed that shear deformation is negligible.

Figure 2 (a) shows the downstream end of a cambered web running under tension between parallel rollers. It is reasonable to expect that tension will stretch the web in a manner that will straighten it. The drawing shows it as straight, but it could have some residual curvature. It is also reasonable to assume that the web will have higher tension on the short edge (left) than on the long edge. In other words, there will be a net moment (negative in this example) on the web that reduces its camber.

---

[4] There are many places where derivatives of y apply only at $x = 0$ or $x = L$. In those cases, partial derivatives evaluated at those locations will be written as ordinary derivatives with subscripts 0 and L. For example, $\left.\frac{\partial y}{\partial x}\right|_{x=L}$ *will be written as* $\frac{dy_L}{dx}$.

Consideration of mass flow makes it clear that this cannot represent a steady state. The tension profile will cause mass to increase on the left-hand side and decrease on the right. So, a boundary defect, β, will develop and change with time.

<u>Figure 2 (b)</u> shows the effect of mass flow on the shape of the relaxed web.

<u>Figure 2 (c)</u> shows the modified edge of the web after it is returned to the line of contact of the roller. It is apparent that original face (before the boundary defect developed) is offset from the roller axis by the boundary defect angle β.

Thus, the effect of the shape change can be approximated by defining the bending angle boundary condition as the boundary defect angle β plus the roller angle applied to the original reference shape. So,

$$\phi_L = \beta + \gamma_L \tag{34}$$

The pivoting motion of the roller is not necessarily in the plane of the web span, so γ_L is the projection of the roller angle onto the plane of the web.

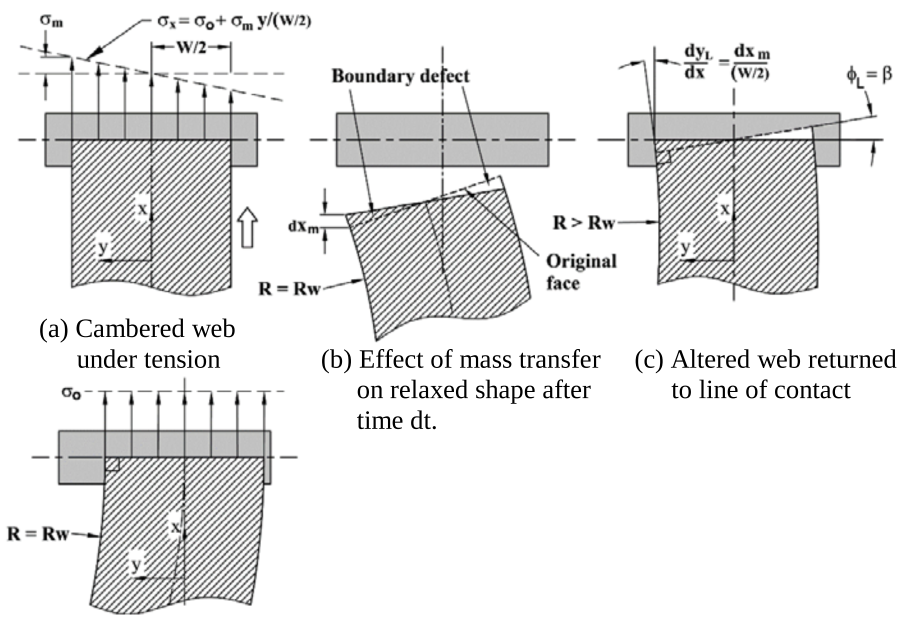

(a) Cambered web under tension

(b) Effect of mass transfer on relaxed shape after time dt.

(c) Altered web returned to line of contact

(d) Steady state

Figure 2 – Effect of Mass Flow on Downstream Boundary for Cambered Web (without Shear)

<u>Figure 2 (d)</u> shows the web after it has moved to the right, under the influence of β. It eventually reaches a position where the curvature of the web (while it is running, under tension) is the same as for the relaxed web. At that point, the moment will be zero, β will be zero and the entry angle will be zero. So, the web will be in a steady state.

The boundary defect angle β can be calculated as follows.

Analysis of the Effect of Mass Transfer (Includes Shear Deformation)

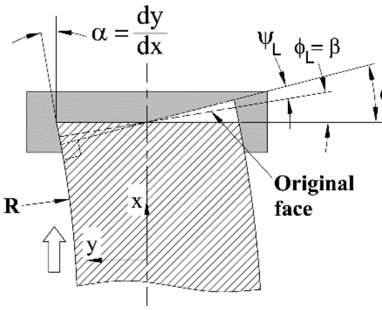

Figure 3 – Relationship between Slope and Bending with Shear

The calculation of β is the same as for a uniform web, except for the definition of moment. The effect of

$$dx_m = V_o\, dt\, \varepsilon_m \tag{35}$$

where ε_m is the increment of strain due to σ_m and V_o is the transport velocity.

The rate of change of the boundary defect angle β can now be calculated, using {35}.

$$\frac{d\beta}{dt} = \frac{dx_m}{dt}\frac{1}{W/2} = 2\frac{\varepsilon_m V_o}{W} \tag{36}$$

Next, we calculate β in terms of the moment. This can be done by finding an expression for curvature in terms of ε_m. The negative moment M is first expressed in terms of the stress profile as,

$$M = -\int_{-W/2}^{W/2} y\left(\sigma_o + \sigma_m \frac{2y}{W}\right) h\, dy = \frac{-W^2 h \sigma_m}{6} = \frac{-W^2 h\, \varepsilon_m E}{6} \tag{37}$$

The moment for a cambered web is by definition,

$$M = EI\left(a\frac{d^2 y_L}{dx^2} - \frac{1}{R_w}\right) = E\frac{W^3 h}{12}\frac{d^2 y_L}{dx^2} \tag{38}$$

Equating {37} to {38} and solving for the curvature,

$$\left(a\frac{d^2 y_L}{dx^2} - \frac{1}{R_w}\right) = -2\frac{\sigma_m}{EW} = -2\frac{\varepsilon_m}{W} \tag{39}$$

Using equations {36} and {39} ,

$$\frac{d\beta}{dt} = -V_o\left(a\frac{d^2 y_L}{dx^2} - \frac{1}{R_w}\right) \tag{40}$$

Taking the time derivative of {34} and substituting {40},

$$\frac{d\phi_L}{dt} = -V_o\left(a\frac{d^2y_L}{dx^2} - \frac{1}{R_w}\right) + \frac{d\gamma_L}{dt} \qquad \{41\}$$

This is the mass transfer equation for a cambered web.

The Acceleration Equation

The acceleration equation is derived by first taking the time derivative of the shape equation for slope {26}.

$$\frac{d}{dt}\frac{dy_L}{dx} = \left(\frac{dy_0}{dt} - \frac{dy_L}{dt}\right)\frac{h_1}{L} + \frac{d}{dt}\left(\phi_L + \chi_L\right)h_2 + \frac{d}{dt}\left(\phi_0 + \chi_0\right)h_3 \qquad \{42\}$$

Then, $d\phi_L/dt$ is replaced using {41} and the cross derivative is replaced using the time derivative of the velocity equation {33}. The result is,

$$\frac{d^2y_L}{dt^2} = V_o^2\left(a\frac{d^2y_L}{dx^2} - \frac{1}{R_w}\right)h_2 + V_o\left[\left(\frac{dy_L}{dt} - \frac{dy_o}{dt}\right)\frac{h_1}{L} + \frac{d\gamma_L}{dt}\left(1-h_2\right) - \frac{d\phi_0}{dt}h_3\right] + \frac{d^2z_L}{dt^2} \qquad \{43\}$$

This is the acceleration equation for a cambered web with shear. It is the same as for a uniform web, except for the $1/R_w$ term.

The meaning of β

Equating values of ϕ_L, from {34} and {1},

$$\gamma_L - \frac{dy_L}{dx} = -\beta - \psi_L - \chi_L \qquad \{44\}$$

Substituting the right side of {44} for the entry angle in the velocity equation {33} yields,

$$\frac{dy_L}{dt} = V_o\left(-\beta - \psi_L - \chi_L\right) + \frac{dz_L}{dt} \qquad \{45\}$$

Thus, the lateral velocity is zero only when $\beta = -\psi_L - \chi_L$ and it can be shown, using {26} and {41}, that the time derivative of {45} is equivalent to the acceleration equation {43}.

THE MULTI-SPAN DIFFERENTIAL EQUATION FOR A CAMBERED WEB

A differential equation for lateral displacement at the downstream end of a cambered web may be created by first solving the slope equation {26} for ϕ_L and substituting the result into the curvature equation {27}. Then, the velocity equation {33} and the acceleration equation {43} are used to replace the first and second order spatial derivatives with time derivatives.

The resulting cambered web model is,

$$\frac{d^2 y_L}{dx^2} = \left(y_0 - y_L\right)\frac{a}{\tau^2}\left(g_1 h_2 - h_1 g_2\right) + \frac{dy_L}{dt}\frac{1}{\tau}\left(h_1 - g_2 a\right) - \frac{dy_0}{dt}\frac{h_1}{\tau} - \frac{h_2 V_o^2}{R_w} - \frac{d^2\phi_o}{dt}V_o h_3$$
$$+\left(\phi_0 - \frac{x_o}{R_w}\right)\frac{aV_o}{\tau}\left(g_3 h_2 - h_3 g_2\right) + \gamma_L \frac{g_2 a V_o}{\tau} + \frac{d\gamma_L}{dt}V_o\left(1-h_2\right) + \frac{dz_L}{dt}\frac{g_2 a}{\tau} + \frac{d^2 z_L}{dt^2} \qquad \{46\}$$

In transfer function form,

$$y_L(s) = \frac{-\frac{h_1}{\tau}s + \frac{a}{\tau^2}\left(g_1 h_2 - g_2 h_1\right)}{s^2 + \frac{1}{\tau}\left(a g_2 - h_1\right)s + \frac{a}{\tau^2}\left(g_1 h_2 - g_2 h_1\right)} y_0(s) + \frac{-V_o h_3 s + \frac{V_o a}{\tau}\left(g_3 h_2 - g_2 h_3\right)}{s^2 + \frac{1}{\tau}\left(a g_2 - h_1\right)s + \frac{a}{\tau^2}\left(g_1 h_2 - g_2 h_1\right)}\phi_0(s)$$
$$+\frac{V_o s\left(1-h_2\right) + \frac{V_o}{\tau}a g_2}{s^2 + \frac{1}{\tau}\left(a g_2 - h_1\right)s + \frac{a}{\tau^2}\left(g_1 h_2 - g_2 h_1\right)}\gamma_L(s) + \frac{s^2 + \frac{a}{\tau}g_2 s}{s^2 + \frac{1}{\tau}\left(a g_2 - h_1\right)s + \frac{a}{\tau^2}\left(g_1 h_2 - g_2 h_1\right)} z_L(s) \qquad \{47\}$$
$$+\frac{-V_o \frac{x_o}{R_w}\frac{a}{\tau}\left(g_3 h_2 - h_3 g_2\right) - \frac{V_o^2 h_2}{R_w}}{s^2 + \frac{1}{\tau}\left(a g_2 - h_1\right)s + \frac{a}{\tau^2}\left(g_1 h_2 - g_2 h_1\right)}$$

Except for the last term, equation {47} is the same as found for a uniform web and, as would be expected, the last term disappears when $R_w = \infty$.

THE REFERENCE SHAPE FOR A CAMBERED WEB AND ITS EFFECT ON BOUNDARY CONDITIONS

Orienting the Reference Configuration

In the derivation of the differential equation {46} there is a problem that has been glossed over. We readily accept that a uniform moving web may be modeled as a static rectangular sheet because material that leaves the span is replaced by an identical piece that moves in behind it. Analysis of the effects of mass flow has changed that a bit, but a strategy was found that allows us to continue to treat the reference shape as a static rectangle. In the case of a cambered web, it is less clear how the reference shape should be modeled.

The reference shape enters into the differential equation only as a contribution to slope. So, the solution isn't affected by the absolute position or orientation of it. The O.D.E. makes a rigid body adjustment that correctly positions the solutions, provided that the entry and exit shape angles are correctly specified in the boundary conditions. This requires an adjustment when crossing rollers because the shape angle is discontinuous, as is apparent in Figure 4.

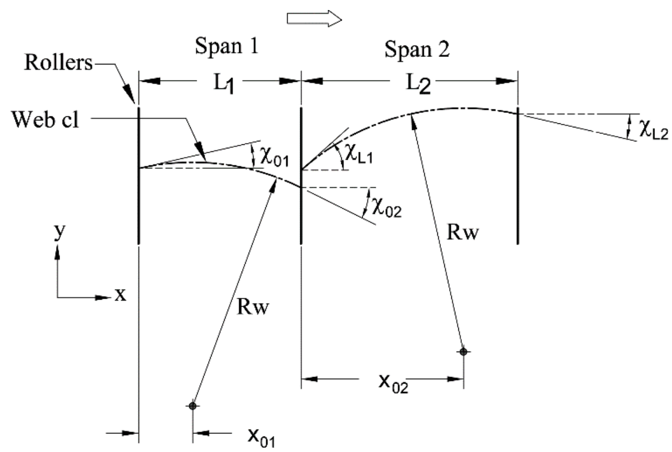

Figure 4 – Possible Reference Shapes for Cambered Web Analysis

In this diagram,

$$\chi_{01} = -\frac{x_{o1}}{R_w} \qquad \chi_{L1} = \frac{L_1 - x_{o1}}{R_w} \qquad \chi_{02} = -\frac{x_{o2}}{R_w} \qquad \chi_{L2} = \frac{L_2 - x_{02}}{R_w} \tag{48}$$

The constant, $x_{o,}$ can be set to zero for all spans.

Specifying ϕ_0

The first two terms of {47} depend on the previous span. The upstream lateral displacement, y_0, is equal to y_L from the previous span. That connection is obvious and straightforward, since lateral position is the primary variable of interest. However, the meaning of ϕ_0 is less clear. It helps to expand on it a bit.

First, we evaluate the boundary defect of the previous span, β^*.

$$\phi_L^* = \frac{dy_L^*}{dx} - \psi^* - \chi_L^* = \beta^* + \gamma_L^* \tag{49}$$

where the stars indicate values in the previous span. So, {49} becomes

$$\beta^* = \frac{dy_L^*}{dx} - \psi^* - \gamma_L^* - \chi_L^* \tag{50}$$

Expression {50} is the boundary defect for the downstream end of the previous span. The slope of the relaxed web, χ, must correspond to the span in which it is used. So, before it can be applied to the upstream end of the current span, χ_L^* must be changed to χ_0. Therefore, the expression for ϕ_0 becomes,

$$\phi_0 = \beta^* + \chi_L^* - \chi_0 + \gamma_0 \tag{51}$$

The shear, ψ, may be calculated from equation {52} using {28},

$$\psi = -\frac{EIn}{AG} a \frac{d^3 y_L}{dx^3} \qquad \{52\}$$

STEADY STATE SOLUTION

If all the time-dependent terms in {46} are eliminated, the steady state solution is found to be,

$$y_L = y_0 + \frac{g_2 L}{g_1 h_2 - h_1 g_2} \gamma_L + \left(\phi_0 - \frac{x_o}{R_w} \right) \frac{L\left(g_3 h_2 - h_3 g_2 \right)}{\left(g_1 h_2 - h_1 g_2 \right)} - \frac{h_2 L^2}{R_w a\left(g_1 h_2 - h_1 g_2 \right)} \qquad \{53\}$$

The following quantities will be needed,

$$\phi_L = \frac{x_o - L}{R_w} + \frac{1}{h_2} \gamma_L - \frac{h_3}{h_2} \left(\phi_0 - \frac{x_o}{R_w} \right) - \frac{h_1}{h_2} \frac{\left(y_0 - y_L \right)}{L} \qquad \{54\}$$

$$y(x) = y_0 + \left(y_0 - y_L \right) g_4(x) + \left[\phi_L + \chi(L) \right] g_5(x) + \left[\phi_0 + \chi(0) \right] g_6(x) \qquad \{55\}$$

The reference curve is defined by equation {16}.

A TYPICAL STEADY STATE SOLUTION

A typical steady state result is shown below. This corresponds to Swanson's Run 4 described in the next section: R_w = -150 m, L = 1.52 m, T = 17.8 N, $\phi_0 = x_o/R_w$, and $\gamma_L = \gamma_0 = 0$.

The results make sense. At $x = L$.

$$a \frac{d^2 y_L}{dx^2} = \frac{1}{R_w} \quad , \quad M_L = 0 \quad , \quad \frac{dy_L}{dx} = 0 \qquad and \qquad \phi_L = \beta + \gamma_L = 0.01 radian \qquad \{56\}$$

Note, that in the steady state, the boundary defect β does not decay to zero. It takes a value that rotates the end of the web to meet the required moment and slope at the roller (zero in both cases).

And y_L = 2.57 mm (toward the long side of the relaxed curve).

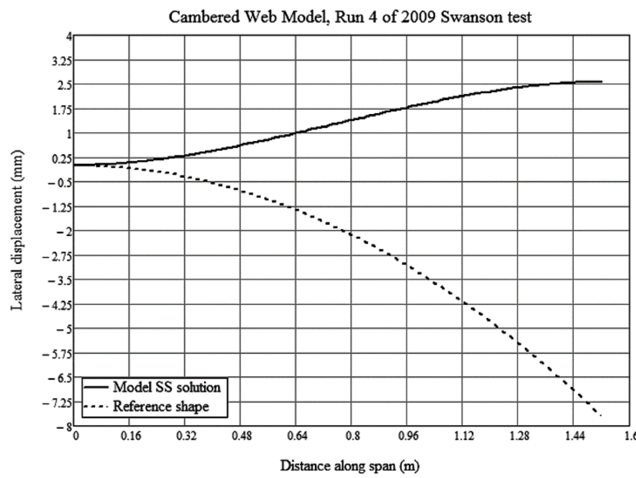

Figure 5 – Steady State Solution for Swanson's Run #4

COMPARISON WITH RON SWANSON'S TESTS

Ron Swanson reported results of a sophisticated test of a cambered web at the 2009 IWEB conference [5]. His machine employed an inline slitting mechanism that cut long sections of with constant camber from an initially straight web. Cambered sections were separated by straight sections for comparison. The chord length of the cambered sections ranged from 9 to 14 meters with radii ranging from 150 to 400 meters. The test span length was adjustable from 1.52 to 3.05 meters. Other web parameters were,

Web material	PET
Thickness	50 μm
Width	0.1524 m
Modulus	4482 MPa
Speed	0.127 m/s
Roller diameter	75 mm

Table 1 – Web Parameters

The test span of the machine was preceded by a displacement web guide that held the edge position constant. The rollers at the ends of the span were fixed and parallel. As a cambered section entered the test span there was an initial disturbance, but the web could achieve a steady state before reaching the end. Rollers were aluminum with an 8 μm finish.

Initial results were not very interesting. The cambered sections seemed to run almost exactly like the uniform sections. There was no significant lateral displacement at the downstream end.

It was discovered, however, that when the rollers in the test span were covered with high friction tape, the web developed a lateral offset of several millimeters at the downstream end in the direction of the long side.

Model outputs are compared with Swanson's results in Table 2. Only those test runs that produced significant offsets were compared. Results were as follows.

			Covering	Covering		y(L)	y(L)	% diff	Φo	ΦL	Side Force
Run	Rw (m)	Span (m)	Upstream	Downstream	T(N)	Exp. (mm)	Model (mm)	Diff./model	Model	Model	Model (N)
4	-150	1.52	3M 5461	3M 5461	17.8	1.478	2.566	42.4	0	0.010076	-0.616
5	-150	1.52	3M 5461	3M 5461	35.6	0.302	2.537	88.1	0	0.01007	-0.645
6	-150	1.52	3M 5461	3M 5461	53.4	0.064	2.51	97.5	0	0.01007	-0.673
7	-150	1.52	Tesa 4863	Tesa 4863	17.8	1.295	2.566	49.5	0	0.010076	-0.616
8	-150	1.52	Tesa 4863	Tesa 4863	35.6	0.919	2.537	63.8	0	0.01007	-0.645
9	-150	1.52	Tesa 4863	Tesa 4863	53.4	0.63	2.51	74.9	0	0.01007	-0.673
13	-300	1.52	3M 5461	3M 5461	17.8	0.813	1.283	36.6	0	0.005038	-0.308
14	-300	1.52	3M 5461	3M 5461	35.6	0.114	1.269	91.0	0	0.005366	-0.322
17	-400	3.05	Tesa 4863	Tesa 4863	17.8	1.364	3.731	63.4	0	0.007613	-0.132
18	-400	3.05	Tesa 4863	Tesa 4863	35.6	1.24	3.592	65.5	0	0.007611	-0.152
19	-400	3.05	Al	Tesa 4863	17.8	1.4	3.731	62.5	0	0.007613	-0.132
20	-400	3.05	Al	Tesa 4863	35.6	1.052	3.592	70.7	0	0.007611	-0.152
24	150	1.52	3M 5461	3M 5461	17.8	-1.44	-2.566	43.9	0	-0.01008	0.616
25	150	1.52	3M 5461	3M 5461	35.6	-0.302	-2.537	88.1	0	-0.01007	0.645
26	150	1.52	3M 5461	3M 5461	53.4	-0.0762	-2.51	97.0	0	-0.01007	0.673

Table 2 – Comparison with Swanson's Tests

An important piece of input data is not available in Swanson's results. There is no value for ϕ_0. An assumed value of zero was used to get the data of Table 2 ($x_o = 0$), but there is no way of knowing if this is correct. To get some idea of the effect of non-zero values of ϕ_0, its value was adjusted until the model agreed with the test data. The results are shown in Table 3.

			Covering	Covering	y(L)	y(L)	y(L)	Φo	ΦL	Force
Run	Rw (m)	Span (m)	Upstream	Downstream	Exp. (mm)	Model (mm)	Model	Model	Model	Model
4	150	1.52	3M 5461	3M 5461	17.8	1.478	1.476	-0.00221	0.010100	-0.737
5	150	1.52	3M 5461	3M 5461	35.6	0.302	0.304	-0.00588	0.010040	-0.952
6	150	1.52	3M 5461	3M 5461	53.4	0.064	0.064	-0.00517	0.010046	-0.93
7	150	1.52	Tesa 4863	Tesa 4863	17.8	1.295	1.295	-0.00258	0.010060	-0.757
8	150	1.52	Tesa 4863	Tesa 4863	35.6	0.919	0.919	-0.00335	0.010570	-0.82
9	150	1.52	Tesa 4863	Tesa 4863	53.4	0.63	0.63	-0.00397	0.010052	-0.871
13	300	1.52	3M 5461	3M 5461	17.8	0.813	0.814	-0.000942	0.005032	-0.372
14	300	1.52	3M 5461	3M 5461	35.6	0.114	0.114	-0.00239	0.005025	-0.447
17	400	3.05	Tesa 4863	Tesa 4863	17.8	1.364	1.364	-0.00253	0.007610	-0.161
18	400	3.05	Tesa 4863	Tesa 4863	35.6	1.24	1.24	-0.0027	0.007608	-0.178
19	400	3.05	Al	Tesa 4863	17.8	1.4	1.4	-0.00249	0.007610	-0.161
20	400	3.05	Al	Tesa 4863	35.6	1.052	1.052	-0.00292	0.007608	-0.18
24	150	1.52	3M 5461	3M 5461	17.8	-1.44	-1.44	0.002282	-0.010064	0.741
25	150	1.52	3M 5461	3M 5461	35.6	-0.302	-0.302	0.004629	-0.010051	0.887
26	150	1.52	3M 5461	3M 5461	53.4	-0.0762	-0.076	0.005143	-0.010050	0.929

Table 3 – Values of ϕ_0 that Would Produce Agreement with the Tests

The values of ϕ_0 found this way ranged from 0.0021 radians (0.12 degree) to 0.005 radians (0.3 degree). This shows that the results are very sensitive to ϕ_0 and would have been difficult to observe by eye.

Swanson evaluated the relative importance of traction at the upstream and downstream ends by running tests in which only one end was taped. This indicated that it was more important to have traction downstream rather than upstream. On the other hand, it was noticed that there was some evidence of circumferential slipping on one end of the upstream roller (shown in Figure 20 of the Swanson paper).

CONCLUSIONS

It has been shown how the mass transfer concept can be applied to nonuniform webs and the specific case of the cambered web has been worked out in detail.

Steady state results agree qualitatively with Swanson's 2009 results [5] and are of the correct order of magnitude.

REFERENCES

1. Shelton, J. J., "Lateral Dynamics of a Moving Web," PhD Thesis, Oklahoma State University, July 1968 .
2. Brown, J. L., "Effect of Mass Transfer on Multi-Spam Lateral Dynamics of a Uniform Web," Proceedings of the Fourteenth International Web Handling Conference, June 2017.
3. Sievers, L., "Modeling and Control of Lateral Web Dynamics," PhD Thesis, Rensselaer Polytechnic Institute, Troy, NY, 1987
4. Benson, R. C., "Lateral Dynamics of a Moving Web With Geometrical Imperfection," ASME Journal of Dynamic Systems, Measurement, and Control, Vol. 124, March 2002.
5. Swanson, Ronald P., "Lateral Dynamics of a Non-Uniform Web," Proceedings of the Tenth International Conference on Web Handling, June, 2009.